

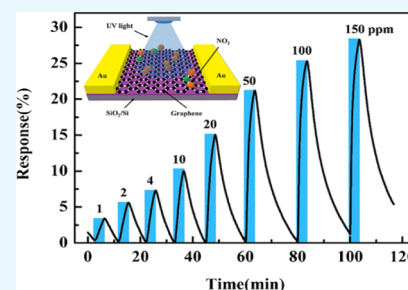
High-Performance UV-Assisted NO₂ Sensor Based on Chemical Vapor Deposition Graphene at Room Temperature

Xin Yan,[†] Yanan Wu,[†] Rui Li,[†] Chengqian Shi,[†] Ramiro Moro,[†] Yanqing Ma,^{*,†,‡,§,||} and Lei Ma^{*,†,||}

[†]Tianjin International Center for Nanoparticles and Nanosystems and [‡]State Laboratory of Precision Measuring Technology and Instruments, Tianjin University, Tianjin 300072, China

Supporting Information

ABSTRACT: Nitrogen dioxide (NO₂) is one of the most dangerous air pollutants that can affect human health even at the ppb (part per billion) level. Thus, the superior sensing performance of nitrogen dioxide gas sensors is an imperative for real-time environmental monitoring. Traditional solid-state sensors based on metal-oxide transistors have the drawbacks of high power consumption, high operating temperature, poor selectivity, and difficult integration with other electronics. In that respect, graphene-based gas sensors have been extensively studied as potential replacements. However, their advantages of high sensing efficiency, low power consumption, and simple electronic integration have been countered by their slow response and poor repeatability. Here, we report the fabrication of high-performance ultraviolet (UV)-assisted room temperature NO₂ sensors based on chemical vapor deposition-grown graphene. UV irradiation improves the response of the sensor sevenfold with respect to the dark condition attaining 26% change in resistance at 100 ppm NO₂ concentration with a practical detection limit below 1 ppm (42.18 ppb). In addition, the recovery time was shortened fivefold to a few minutes and the excellent repeatability. This work may provide a promising and practical method to mass produce room-temperature NO₂ gas sensors for real-time environment monitoring due to its simple fabrication process, low cost, and practicality.



INTRODUCTION

Gases NO₂, SO₂, H₂S, CO, H₂, and CH₄ in the atmosphere can seriously threaten the safety and health of human beings.^{1–3} Nitrogen dioxide (NO₂), in particular, which is produced by combustion of fossil fuels, can affect human health even at the ppb (part per billion) level.^{2–4} Therefore, real-time environmental monitoring with gas sensors has become much important in our daily life. Meanwhile, gas sensors also play an important role in medical diagnosis, industrial safety, and food quality control.^{5–8} This has been the motivation in recent years for the progress in the research on gas sensors.^{6,9}

Traditional solid-state gas sensors based on metal oxide semiconductors have low cost and high sensitivity.⁸ Nevertheless, their performance still has the shortcomings of high operating temperatures, high power consumption, poor selectivity, low integration degree, and poor long-term stability. Hence, it is an important goal to improve the performance of next generation of gas sensors. Desirable qualities include high sensitivity, low detection limit, fast response and recovery time, high integration degree, room-temperature operation, and low energy consumption.¹⁰

Novel nanostructured materials with small volume and specific structures have demonstrated extraordinary potential for application as sensing layers.^{2,11–14} As a member of two-dimensional materials, graphene has been the subject of intensive research because of its excellent physical and chemical properties,^{15–17} including its single-atom thickness,

unique energy band structure, outstanding electrical properties, high carrier mobility,¹⁸ large surface-to-volume ratio, and great thermal conductivity.¹⁹

Graphene has great prospects in the fields of biology, chemistry, machinery, aviation, and military.^{16,20,21} For gas sensors,^{22,23} compared to conventional devices graphene has the advantage of maximum surface area per unit volume because of its ultrathin flake structure only one atom thick (~0.34 Å).¹⁵ All the carbon atoms in graphene are exposed to the target gas molecules, which can yield high sensing efficiency.²² Also, even in the limit of few charge carriers, a small amount of extra electrons can cause a large change in the conductance of graphene because of its low Johnson noise.²⁴ Last, graphene devices possess higher conductivity compared with metal oxide-based gas sensors, so they can be more suitably integrated with actual electronic circuits.^{2,23} However, the electrical properties of graphene are heavily dependent on the synthesis method and quality of lattice.¹⁶ In graphene synthesized by the micromechanical cleavage of graphite, it is difficult to control the thickness and area of the films, which is unsuitable for mass production.²⁵ Epitaxial graphene can be used to prepare graphene devices, but its high production cost restricts wide applications.^{26–29} Graphene oxides or reduced graphene oxide synthesized by chemical methods usually have

Received: April 2, 2019

Accepted: August 9, 2019

Published: August 22, 2019

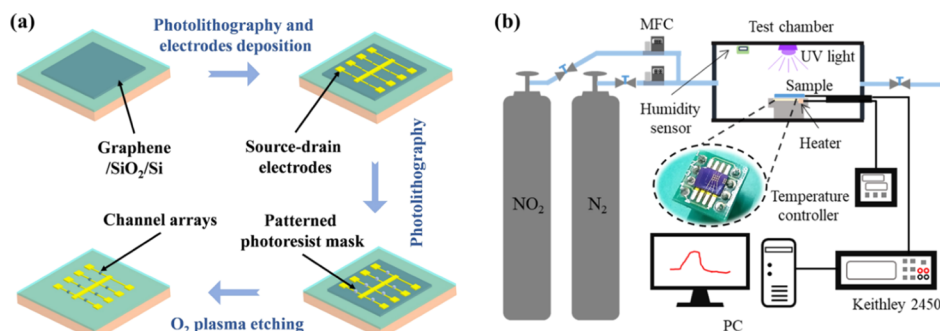


Figure 1. (a) Fabrication process for the graphene gas sensor. (b) Schematic illustration of the test system for gas sensing. The inset shows the image of the graphene sensor arrays binding with chip carrier.

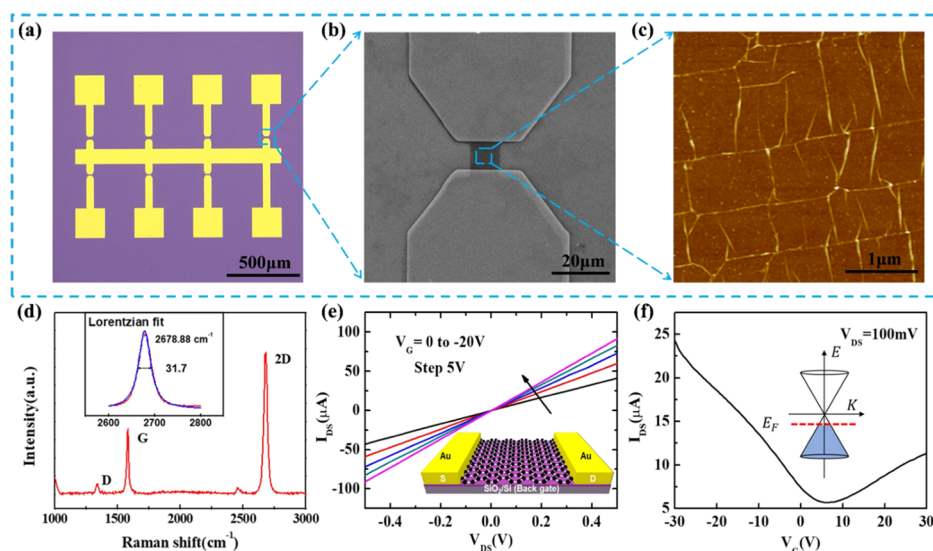


Figure 2. (a) Optical image of graphene-based sensor arrays on the SiO₂/Si substrate. (b) SEM image of an individual gas sensor device. (c) AFM image of the patterned clean graphene surface. (d) Raman spectrum of the patterned graphene channel, and the inset shows the schematic illustration of the graphene FETs, where the Si substrate was used as the gate electrode. (e) Current–voltage (*I*-*V*) curves of the graphene-based sensors, and the inset shows the schematic illustration of the graphene FETs, where the Si substrate was used as the gate electrode. (f) Current–gate voltage (*I*-*V*_G) transfer curve exhibited an ambipolar behavior with a charge neutral point near *V*_G ≈ 5 V. The inset shows simplified band structure near the K points and Fermi level-dependent charge carrier concentration. p-type doping can create hole-like charge carriers.

poor conductivity.^{30–32} Chemical vapor deposition (CVD)-grown graphene has high crystal quality, excellent electronic properties, and can transfer onto arbitrary substrates,^{33–35} so it is the best candidate material for fabricating graphene devices compared with other methods.

Herein, we report the fabrication of miniature gas sensor arrays based on transferred CVD-grown graphene to detect NO₂ gas at room temperature. The sensing performance, including responsivity, recovery time, detection limit, repeatability, thermal stability, and selectivity were measured and discussed. Initially, the as-prepared gas sensors exhibited weak response and incomplete recovery in dark conditions. As previously reported, the UV irradiation is a feasible means to improve the sensing performance.^{36–39} Then, we tested assisting the gas sensor with UV irradiation at room temperature. With the UV irradiation, the gas sensor has a high response (26% change in resistance) to nitrogen dioxide at 100 ppm, a sevenfold improvement over the dark condition, and this response has a monotonic relationship with gas concentration that can be modeled with piecewise linear functions. In addition, excellent repeatability and weak temperature dependence were observed. These miniature gas

sensor arrays have simple fabrication processes and they can be used in the field of low-concentration nitrogen dioxide detection for real-time environment monitoring.

RESULTS AND DISCUSSION

Characterization of the Graphene-Based Sensor. The graphene-based sensor arrays were fabricated on the SiO₂/Si substrate as shown in Figure 1a. The details of the process were described in the Experimental Section. The mesoscopic morphology of the graphene-based sensors was characterized as shown in Figure 2. The optical image of graphene-based sensors array on the SiO₂/Si substrate is shown in Figure 2a. This array has seven gas sensor devices with a shared electrode. Figure 2b shows the scanning electron microscopy (SEM) image of an individual gas sensor device. Both length and width of the channel are almost 10 μm. Figure 2c shows the atomic force microscopy (AFM) image of the patterned graphene surface. The patterned graphene films with clean surfaces, being a key for high sensitivity, eliminated the influence of contamination and impurities.³³

Raman spectroscopy measurements were used to identify the crystal quality of the transferred CVD-grown graphene and

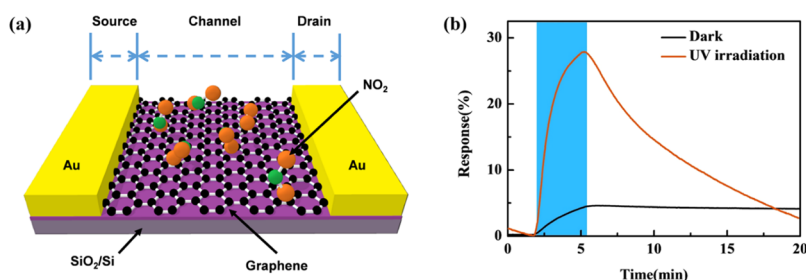


Figure 3. (a) schematic illustration of the sensor based on CVD graphene in the atmosphere containing nitrogen dioxide. (b) response and recovery curves of relative resistance changes of the graphene sensors exposed to 100 ppm concentration of NO_2 gas with and without UV irradiation.

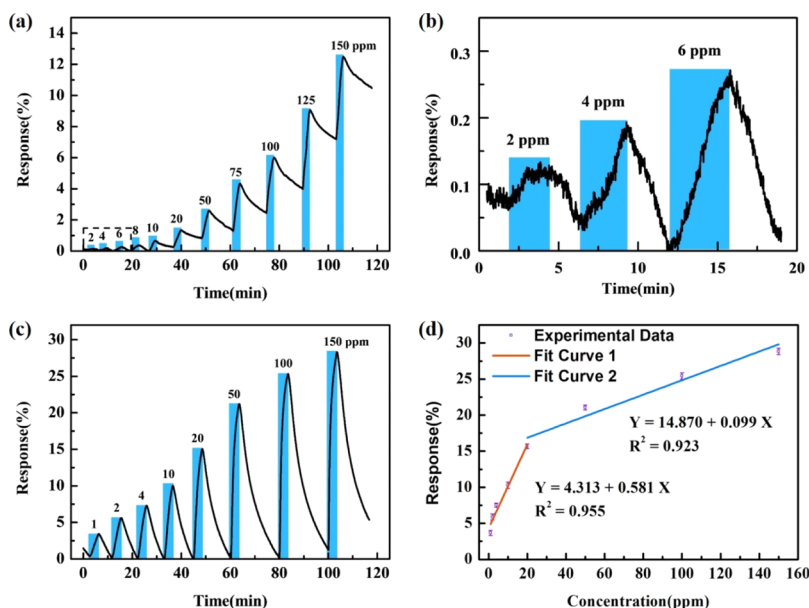


Figure 4. (a) Response and recovery curves of the graphene-based sensor in NO_2 concentration modulated from 2 to 140 ppm in dark conditions. (b) Response and recovery curves of the graphene-based sensor at NO_2 concentrations of 2, 4, and 6 ppm, respectively, in dark conditions. (c) Response and recovery curves of the graphene-based sensor in different NO_2 concentration (modulated from 1 to 150 ppm) under UV irradiation. (d) Fit curves of the response value as a function of NO_2 concentration at room temperature with UV irradiation.

to analyze potential damage introduced through impurities or edge defects.^{40–42} The Raman spectra were obtained using an Andor system with a 532 nm laser. Figure 2d shows the Raman spectrum of the patterned graphene. The Raman spectrum showed typical G peak around $\sim 1583 \text{ cm}^{-1}$. The 2D peaks at $\sim 2679 \text{ cm}^{-1}$ with a full width at half maximum of 31.7 cm^{-1} . The 2D/G intensity ratio was about 2.2, which indicated the patterned graphene is a monolayer.^{35,43} In addition, the patterned graphene exhibited an additional D peak at $\sim 1350 \text{ cm}^{-1}$, which was ascribed to generated edges or defects during the patterning or transfer processes.^{35,44,45}

Electrical transport properties of the graphene-based sensor were measured at room temperature via four-probe station. Figure 2e shows the current–voltage (I – V) curves of the graphene-based sensor applying different gate voltages. The linear ohmic behaviors of I – V curves indicate the high electrical conductivity in our graphene-based sensor for gas-sensing experiments. The current–gate voltage (I – V_G) transfer curve shows an ambipolar behavior with the charge neutral point at $V_G \approx 5 \text{ V}$, as shown in Figure 2f. The n-type silicon substrate was used as the gate electrode. It indicates a slightly p-type doping in the transferred graphene, which is derived from the adsorption of oxygen and water vapor onto

the surface of graphene in the atmosphere during the testing process.^{46,47}

NO_2 Gas Sensing Properties of the Graphene-Based Sensor. As previously reported, graphene-based materials demonstrated tremendous potential for detecting small-molecule gases, for example, NO_2 , NH_3 , CO_2 , H_2O , and SO_2 .^{48–57} Herein, the gas-sensing performance of graphene sensor arrays were detected by choosing NO_2 as the target gas at room temperature. The sensing performance test used a home-made measurement system, as shown in Figure 1b. The details of parameters were described in the Experimental Section.

The response of the sensor is defined as

$$R = \left| \frac{R_g - R_0}{R_0} \right| \times 100\% \quad (1)$$

where R_0 and R_g are the sensor resistances before and after the exposure to NO_2 , respectively. The response time is defined as the time taken for the sensor to achieve 90% of its maximum resistance change, and the recovery time is the time for the resistance to go down to 10% of the maximum resistance change.^{58–60}

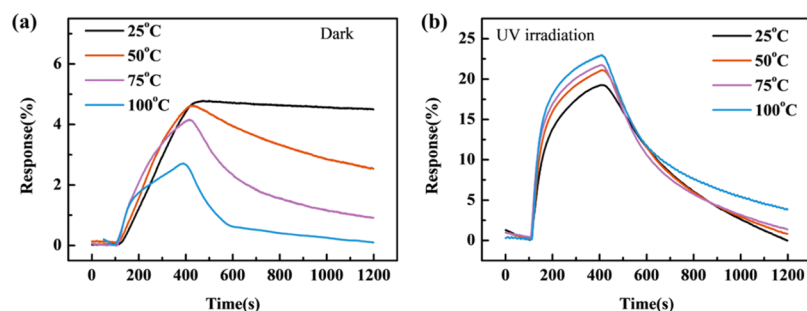


Figure 5. Thermal stability tests of the graphene-based sensor exposed to NO₂ concentrations of 100 ppm at room temperature in (a) dark and (b) UV irradiation.

Fast response and complete recovery are essential to realize high-performance NO₂ gas sensors.⁹ Figure 3a shows schematic illustration of the graphene-based sensor in a complex atmosphere containing nitrogen dioxide. Figure 3b displays the response and recovery curves of the graphene sensor exposed to 100 ppm concentration of NO₂ gas at room temperature toward different conditions. The electrical resistance of the sensor with graphene-sensing layer decreases upon NO₂ molecular adsorption. The electrons transfer from graphene to NO₂ molecule as an electron acceptor.²³ As given in Figure 3b, the graphene-based sensor in the dark condition not only has low response but is also extremely difficult to recover. To improve the response and recovery characteristics, the sensor was irradiated with UV light.^{61,62} The UV source parameters such as wavelength and irradiance will affect the improvement of sensing performance.⁶³ Therefore, the effects of different light wavelengths and irradiance on the sensing performance were systematically investigated. Figure S1 shows the response and recovery curves of the graphene-based sensor exposed to NO₂ under the different light wavelengths. The response and recovery rate were accelerated with decreasing light wavelength. After that, the effects of light (265 nm) irradiance in the range of 0.5–1.7 mW/cm² on the response and recovery of the graphene-based sensor for NO₂ is shown in Figure S2. There is a maximum response under irradiance of 1.21 mW/cm², but the recovery was lower than that of 1.68 mW/cm². For best improvement, the optimum wavelength (265 nm) and irradiance (1.68 mW/cm²) were selected for the following studies. As the red line shown in Figure 3b, the graphene-based sensor under UV irradiation after the NO₂ gas was injected for 200 s, resulted in the maximum response of 26%, which is more than sevenfold that of the graphene sensor in dark conditions. Meanwhile, the recovery time was drastically decreased with UV irradiation, compared to dark conditions. The effect of UV irradiation on the response of the gas sensors can be attributed to the cleaning of the graphene surface. Thus, the available active sites will be occupied by nitrogen dioxide molecules.^{64–66} Simultaneously, the UV irradiation can effectively separate charge carriers at the graphene surface for recovery. As previously reported, the use of UV irradiation was designed to avoid damage of the sensor by controlling the intensity and the wavelength of the UV light.⁶⁷

Based on the abovementioned measurements, the effect of UV light on the correlation between sensing response and concentration was investigated. Figure 4 reveals the real-time response of the graphene sensor with and without UV irradiation measured at different concentrations of NO₂ gas. The response performance of the sensor varied with the

changes in the NO₂ concentration from 2 to 150 ppm (Figure 4a). Figure 4b gives the enlarged response at low NO₂ concentrations of 2, 4, and 6 ppm, respectively (dashed line in Figure 4a). It is of interest to note that the graphene sensor in the dark condition was unable to visibly detect 2 ppm NO₂, and the response value only made 0.1%. For comparison, the graphene sensor exposed to NO₂ concentrations from 1 to 150 ppm under UV irradiation at room temperature (Figure 4c). Additionally, the extremely low concentration of sub-ppm NO₂ gas was clearly detectable using UV irradiation.¹⁰ In other words, the graphene-based sensor assisted by UV light has much lower detection limit. Figure 4d indicates that the sensing response of the UV-assisted graphene sensor monotonously increases with NO₂ concentrations from 1 to 150 ppm. The plots display a linear behavior below 20 ppm corresponding to high-sensitive mode in relatively low-concentration range of NO₂. When the NO₂ concentration is high enough, the response converts to a different linear dependence with lower slope on concentration, which terms as the low-sensitive mode.⁶⁸ There are two explanations for the change in the above slope. One of the views is the lower slope of higher NO₂ concentration caused by the sensor partial saturation, which leads to the response diverged from previous linearity.^{69–72} Another view is that this conversion derives from the enhancement of scattering events between adsorbed NO₂ molecules and charge carriers. At the relatively low NO₂ concentration range, the adsorption sites for NO₂ are sufficient to respond with high sensitivity, and NO₂ molecule adsorption is too rare to affect charge-transport motions. While a great deal of the adsorption sites for the NO₂ molecule are filled at the relatively high NO₂ concentration range, the scattering effects of the adsorbed NO₂ molecules emerge, resulting in adsorption rate of NO₂ molecules turning out to be lower than that of high-sensitive mode and the increase rate of response becoming smaller.⁶⁸ From these fitted curves, the response of the graphene sensor for any concentration can be calculated a consistent value. According to the IUPAC definition, the signal to noise ratio should be higher than 3.⁷³ By the reported calculation method,⁷⁴ the detection limit is estimated to be 42.18 ppb, which is much lower than that in the dark condition (see Figure 4b).

The recovery of the graphene-based sensor was studied as a function of temperature, which could be changed using the adjustable temperature sample holder. As shown in Figure 5a, the response of graphene-based sensor in the dark condition decreases when temperature increases from 25 to 100 °C, but obtained a faster response rate. At the same time, the recovery time also decreased. It can be explained by the following two factors. First, few NO₂ gas molecules are adsorbed on the

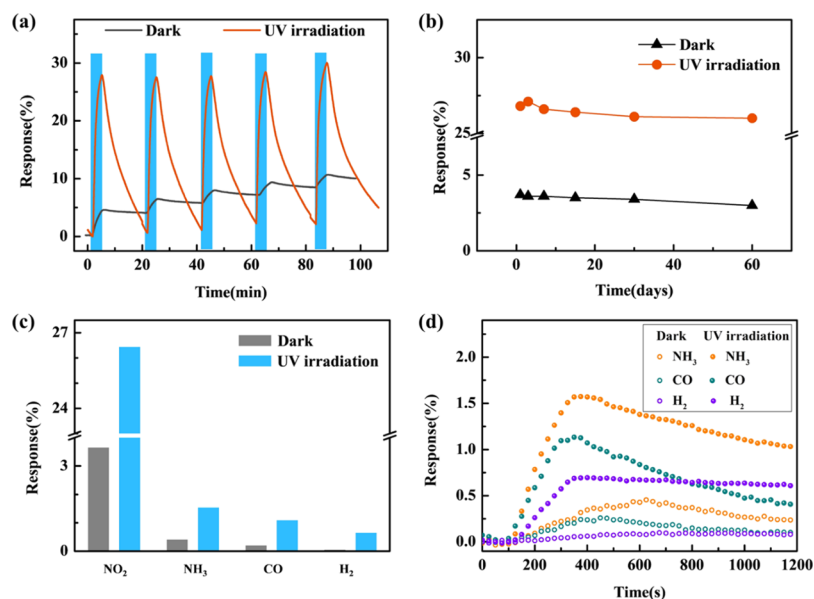


Figure 6. (a) Repeatability and (b) long-term stability tests of the graphene-based sensor exposed to NO_2 concentrations of 100 ppm at room temperature in the dark (black line) and UV irradiation (red line). (c) Selectivity of the graphene-based NO_2 gas sensors in real time toward 100 ppm of different target gases, including NO_2 , NH_3 , CO , and H_2 at room temperature under different light conditions. (d) Response and recovery curves of the graphene-based sensor exposed to NH_3 , CO , and H_2 concentrations of 100 ppm under different light conditions.

graphene surface at high temperature, so the response of the sensor decreased.⁵⁸ Second, high temperature will accelerate the desorption of NO_2 gas molecules from the graphene surface, which results in the decrease of the recovery time.⁵⁸ Figure 5b shows the graphene-based sensor exposed to 100 ppm NO_2 under UV irradiation at different operating temperatures from 25 to 100 °C. The fluctuations of temperature have less effect on the sensing performance under UV irradiation. It indicates that the UV-assisted sensor has better thermal stability than in the dark conditions.

The repeatability of the graphene-based sensor was also investigated by in situ cyclic sensing tests of the graphene-based sensor upon repeated 100 ppm NO_2 exposure and removal. Figure 6a shows the response and recovery curves with five-cycle exposure to 100 ppm NO_2 gas in different conditions. It was observed that the graphene-based sensor under UV irradiation has better repeatability than that in dark conditions. Meanwhile, the response of the UV-assisted graphene sensor has a slight decline (2%) in time of two months (Figure 6b). It means that the good durability and reliability of developing UV-assisted graphene sensors for practical application.

The selectivity of graphene-based sensors which can accurately detect the target gas among other gases is essential characteristic for performance estimation of gas sensors.^{2,11,75} To investigate the selectivity of the NO_2 gas sensor under different conditions, the response of the graphene-based sensor was characterized toward different target gases with 100 ppm at room temperature, including ammonia, carbon oxide, and hydrogen as shown in Figure 6c. Notably, the response toward NO_2 is much higher than NH_3 , CO , and H_2 with the same concentration, implying a favorable selectivity for NO_2 gas detection. Nevertheless, the selectivity of the graphene-based sensor has not been obviously improved with UV irradiation, compared to that in dark condition. Figure 6d shows the response and recovery curves of the graphene-based sensor

exposed to 100 ppm NH_3 , CO , and H_2 under different light conditions.

Gas-Sensing Mechanism of the Graphene-Based Sensor. As verified by previous reports, the sensing mechanism is the charge transfer due to the relative position in the density of state of the highest occupied and lowest unoccupied molecular orbitals [highest occupied molecular orbital and lowest unoccupied molecular orbital (LUMO)] within adsorbate.^{51,76} For NO_2 adsorbed on graphene, the LUMO is situated 0.3 eV below the Dirac point of graphene and independent of adsorption geometry. It demonstrates that the absorption of NO_2 molecules on the graphene surface is van der Waals interactions.⁵¹ Furthermore, we investigated the gas-sensing mechanisms of the graphene-based sensor by testing their resistivity changes because of adsorption or desorption of NO_2 gas molecules,^{22,51,77} which is similar to other solid-state sensors.^{11,76,78} For the graphene-based sensor with slightly p-type doping, NO_2 molecules as electron acceptors are adsorbed on the graphene surface. It can result in the increase of the hole concentrations, leading to the increase conductivity of the sensing layer.

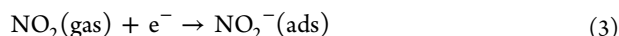
The effects of UV irradiation can be explained by two main respects. On the one hand, UV irradiation-induced desorption of impurity molecules like oxygen or water molecules, then created a host of adsorption sites on the surface for nitrogen dioxide adsorption. On the other hand, the luminous energy of UV light (~ 4.68 eV) exceeds the band gap of p-type graphene, the UV irradiation can excite electron–hole pairs in the p-type graphene-sensing layer. These additional photogenerated electron transfer from the valence band to the conduction band,^{2,64} then participate in the charge transfer.

Before the gas-sensing test, the graphene-based sensor was fabricated in the atmosphere, which unavoidably results in the adsorption of oxygen molecules on the surface of graphene. There will be two parts of these adsorbed oxygen molecules. One portion of oxygen molecules remained physically adsorbed on the graphene surface. The other part of oxygen

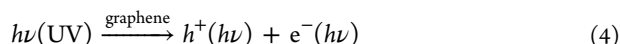
molecules serves as an electron-acceptor because of the oxidizing property. The electrons are attracted to the adsorbed oxygen molecules, which lead to slightly p-type properties of graphene. The reaction process can be written as follows⁷⁹



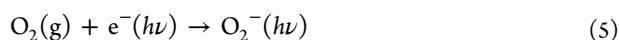
While the sensor is exposed to the NO₂ gas, electrons are further transferred from the p-type graphene to the NO₂ molecules, as a result of the increase of the hole concentrations of the graphene-sensing layer according to the following reaction⁸⁰



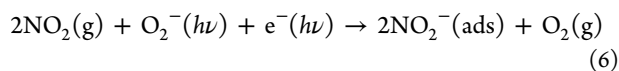
When the UV irradiation was applied, the photogenerated electron–hole pairs appeared in the graphene surface, as shown in the following reaction^{64,79}



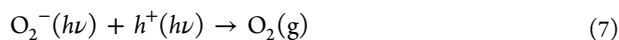
At the same time, photogenerated electrons can combine with oxygen molecules, which can form additional photo-induced oxygen ions O₂[−](hν)^{64,66,81}



Furthermore, a portion of photogenerated electrons e[−](hν) were involved in the reaction with NO₂ molecules, and lead to the larger p-type doping than in the dark condition, according to the following reaction⁶⁶



With the NO₂ gas molecules withdrawn, the achieved balance in eq 5 is broken. The photoinduced oxygen ions O₂[−](hν) will recover to O₂ molecules^{66,82}



Hence, the recovered O₂ molecules were returned to its original state before the NO₂ gas injection and then achieved the repetitive and reversible room-temperature operation.

CONCLUSIONS

In conclusion, graphene-based NO₂ gas sensor arrays that operate at room temperature assisted with UV have been prepared. The graphene-based gas sensor under UV irradiation exhibits high response for the detection of NO₂ gas even at sub-ppm levels, and the response (26% at 100 ppm) is more than sevenfold than that in dark conditions. Meanwhile, the graphene-based gas sensor under UV irradiation has complete recovery, and the recovery time was drastically decreased. Furthermore, the correlation between NO₂ gas concentrations and response characteristic of the graphene-based gas sensor was in good agreement with a piecewise linear relation.

The improvement of sensing performance probably can be explained by several aspects. On the one hand, the UV irradiation provided more favorable active sites for NO₂ gas adsorption. On the other hand, the UV irradiation enhanced the recovery characteristic of the sensor because of the desorption rate of NO₂ molecules accelerated by light energy. In addition, the as-prepared gas sensor also has favorable repeatability, thermal stability, and selectivity. The UV-assisted sensor can be used in a special atmosphere where concentration of dangerous gases higher than the lower explosive limit. Hence, the UV irradiation is a feasible means

to improve the sensing performance of the graphene-based sensor for gas-sensing applications.

EXPERIMENTAL SECTION

Synthesis and Transfer of Graphene. The uniform monolayer graphene was grown on copper foils (25 μm) via atmospheric pressure CVD with CH₄ gas as the carbon source. Before graphene growth, the copper foils were cleaned by diluted hydrochloric acid. Then, rinsed by acetone, ethanol, deionized water, and dried by blowing pure N₂. After that, the dry copper foils were loaded into a CVD system in a horizontal tube furnace with a 2 in. quartz tube. The system was pumped down to a vacuum of 10^{−1} Pa and refilled with pure Ar gas. Then heated to 1050 °C for 60 min. Subsequently, a mixture of diluted methane and hydrogen was introduced into the CVD system for the graphene growth at 1050 °C with CH₄/H₂ molar ratio (0.5:50 sccm) under ambient pressure for 30 min. The growth was terminated with a cooling rate of 25 °C/min in the ambient environment. The graphene was grown on both sides of the copper foils. One side of the graphene/copper surface was spin-coated with PMMA (polymethyl methacrylate). The other side of the copper foils was exposed to oxygen plasma for 30 s to remove the graphene. The transfer of graphene films onto the Si substrate with the 285 nm thick thermally grown SiO₂ layer was performed by the wet-etching of the copper substrates. After that, the Cu foils were etched away using ferric trichloride solution, resulting in the free-standing PMMA/graphene films floating on the surface of the solution. The PMMA/graphene films were cleaned by deionized water, and transferred onto the substrate until they are air dry, then use acetone/acetic acid mixed solution dissolving PMMA films sequentially. Finally, the substrate was cleaned with isopropyl alcohol and deionized water.

Fabrication of Graphene Devices. The graphene-based sensor arrays were fabricated on the SiO₂/Si substrate as shown in Figure 1a. First, photolithography was employed again to pattern the contact electrode area on graphene transferred onto the Si/SiO₂ substrate. Then, the electrodes (10 nm Cr/50 nm Au) were deposited by e-beam evaporation. Second, photolithography was used to pattern channels into 10 μm wide strips. Finally, oxygen plasma etching was used to etch away the redundant graphene. Subsequently, the back gate was applied to the Si substrate. Before the gas-sensing measurements, the sensor array would be connected by a gold wire from the electrodes to the chip carrier via ultrasonic wire bonder.

Gas-Sensing Performance Evaluation. For gas-sensing experiments, we have constructed a home-built measuring system with electrical feedthrough, adjustable temperature sample holder (from room temperature to 150 °C), and UV-LED as shown in Figure 1b. The measurements were performed under atmospheric pressure at controlled temperature (23 ± 2 to 100 °C). To measure the sensing performance, the gas flow was a constant of 1000 sccm (standard cubic centimeter per minute). Various concentrations of target gas were injected into the test chamber by adjusting the flow ratio of target gas to dry N₂ using the mass flow controller. Dry N₂ was separately injected into the chamber for measuring the recovery of the sensor. The UV light is used to investigate the effect of ultraviolet light on sensing performance. The applied bias voltage was fixed at 100 mV during the testing process. The electrical measurements

were carried out using a high-sensitivity SourceMeter (Keithley 2450), which is connected with computer for signal collection.

■ ASSOCIATED CONTENT

● Supporting Information

The Supporting Information is available free of charge on the ACS Publications website at DOI: 10.1021/acsomega.9b00935.

Response and recovery curves of the sensor under the different light wavelengths; response and recovery curves of the sensor under UV light ($\lambda = 265$ nm) with different irradiance; and the effects of light irradiance in the range of 0.5–1.7 mW/cm² on the response and recovery of the sensor (PDF)

■ AUTHOR INFORMATION

Corresponding Authors

*E-mail: mayanqing@tju.edu.cn (Y.M.).

*E-mail: lei.ma@tju.edu.cn (L.M.).

ORCID

Yanqing Ma: 0000-0002-3317-8273

Lei Ma: 0000-0002-2446-4833

Author Contributions

The protocol was designed by X.Y. and L.M. Methodology was performed by X.Y., Y.W., C.S., R.M., Y.M. and L.M. The manuscript was written and revised by X.Y., Y.M. and L.M.

Notes

The authors declare no competing financial interest.

■ ACKNOWLEDGMENTS

This work was financially supported by the National Natural Science Foundation of China (no. 11774255), the Key Project of Natural Science Foundation of Tianjin City (no. 17JCZDJC30100).

■ REFERENCES

- (1) Liu, J.; Li, S.; Zhang, B.; Xiao, Y.; Gao, Y.; Yang, Q.; Wang, Y.; Lu, G. Ultrasensitive and low detection limit of nitrogen dioxide gas sensor based on flower-like ZnO hierarchical nanostructure modified by reduced graphene oxide. *Sens. Actuators, B* **2017**, *249*, 715–724.
- (2) Zhang, J.; Liu, X.; Neri, G.; Pinna, N. Nanostructured Materials for Room-Temperature Gas Sensors. *Adv. Mater.* **2016**, *28*, 795–831.
- (3) Kong, J.; Franklin, N. R.; Zhou, C.; Chapline, M. G.; Peng, S.; Cho, K.; Dai, H. Nanotube molecular wires as chemical sensors. *Science* **2000**, *287*, 622–625.
- (4) Gouveia, N. C.; Maisonet, M. *Health Effects of Air Pollution: An Overview*, 2006.
- (5) Basu, S.; Bhattacharyya, P. Recent developments on graphene and graphene oxide based solid state gas sensors. *Sens. Actuators, B* **2012**, *173*, 1–21.
- (6) Capone, S.; Forleo, A.; Francioso, L.; Rella, R.; Siciliano, P.; Spadavecchia, J.; Presicce, D. S.; Taurino, A. M. Solid State Gas Sensors: State of the Art and Future Activities. *J. Optoelectron. Adv. Mater.* **2003**, *5*, 1335–1348.
- (7) Chatterjee, S. G.; Chatterjee, S.; Ray, A. K.; Chakraborty, A. K. Graphene–metal oxide nanohybrids for toxic gas sensor: A review. *Sens. Actuators, B* **2015**, *221*, 1170–1181.
- (8) Moseley, P. T. Solid state gas sensors. *Mach. Sci. Technol.* **1997**, *8*, 223.
- (9) Liu, S.; Yu, B.; Zhang, H.; Fei, T.; Zhang, T. Enhancing NO₂ gas sensing performances at room temperature based on reduced graphene oxide-ZnO nanoparticles hybrids. *Sens. Actuators, B* **2014**, *202*, 272–278.
- (10) Chen, G.; Paronyan, T. M.; Harutyunyan, A. R. Sub-ppt gas detection with pristine graphene. *Appl. Phys. Lett.* **2012**, *101*, 652–655.
- (11) Donarelli, M.; Ottaviano, L. 2D Materials for Gas Sensing Applications: A Review on Graphene Oxide, MoS₂, WS₂ and Phosphorene. *Sensors* **2018**, *18*, 3638.
- (12) Ray, S. J. First-principles study of MoS₂, phosphorene and graphene based single electron transistor for gas sensing applications. *Sens. Actuators, B* **2016**, *222*, 492–498.
- (13) Liu, X.; Ma, T.; Pinna, N.; Zhang, J. Two-Dimensional Nanostructured Materials for Gas Sensing. *Adv. Funct. Mater.* **2017**, *27*, 1702168.
- (14) Su, Y.; Wu, Z.; Wu, X.; Long, Y.; Zhang, H.; Xie, G.; Du, X.; Tai, H.; Jiang, Y. Enhancing responsivity of ZnO nanowire based photodetectors by piezo-phototronic effect. *Sens. Actuators, A* **2016**, *241*, 169–175.
- (15) Geim, A. K.; Novoselov, K. S. The rise of graphene. *Nat. Mater.* **2007**, *6*, 183–191.
- (16) Geim, A. K. Graphene: Status and Prospects. *Science* **2009**, *324*, 1530.
- (17) Ferrari, A. C.; Bonaccorso, F.; Fal'ko, V.; Novoselov, K. S.; Roche, S.; Bøggild, P.; Borini, S.; Koppens, F. H. L.; Palermo, V.; Pugno, N.; Garrido, J. A.; Sordan, R.; Bianco, A.; Ballerini, L.; Prato, M.; Lidorikis, E.; Kivioja, J.; Marinelli, C.; Ryhänen, T.; Morpurgo, A.; Coleman, J. N.; Nicolosi, V.; Colombo, L.; Fert, A.; Garcia-Hernandez, M.; Bachtold, A.; Schneider, G. F.; Guinea, F.; Dekker, C.; Barbone, M.; Sun, Z.; Galiotis, C.; Grigorenko, A. N.; Konstantatos, G.; Kis, A.; Katsnelson, M.; Vandersypen, L.; Loiseau, A.; Morandi, V.; Neumaier, D.; Treossi, E.; Pellegrini, V.; Polini, M.; Tredicucci, A.; Williams, G. M.; Hee Hong, B.; Ahn, J.-H.; Min Kim, J.; Zirath, H.; van Wees, B. J.; van der Zant, H.; Occhipinti, L.; Di Matteo, A.; Kinloch, I. A.; Seyller, T.; Quesnel, E.; Feng, X.; Teo, K.; Rupesinghe, N.; Hakonen, P.; Neil, S. R. T.; Tannock, Q.; Löfwander, T.; Kinaret, J. Science and technology roadmap for graphene, related two-dimensional crystals, and hybrid systems. *Nanoscale* **2015**, *7*, 4598–4810.
- (18) Bolotin, K. I.; Sikes, K. J.; Jiang, Z.; Klima, M.; Fudenberg, G.; Hone, J.; Kim, P.; Stormer, H. L. Ultrahigh electron mobility in suspended graphene. *Solid State Commun.* **2008**, *146*, 351–355.
- (19) Balandin, A. A.; Ghosh, S.; Bao, W.; Calizo, I.; Teweldebrhan, D.; Miao, F.; Lau, C. N. Superior thermal conductivity of single-layer graphene. *Nano Lett.* **2008**, *8*, 902.
- (20) Bonaccorso, F.; Sun, Z.; Hasan, T.; Ferrari, A. C. Graphene photonics and optoelectronics. *Nat. Photonics* **2010**, *4*, 611–622.
- (21) Chen, Z.; Lin, Y.-M.; Rooks, M. J.; Avouris, P. Graphene nanoribbon electronics. *Phys. E* **2007**, *40*, 228–232.
- (22) Schedin, F.; Geim, A. K.; Morozov, S. V.; Hill, E. W.; Blake, P.; Katsnelson, M. I. Detection of individual gas molecules adsorbed on graphene. *Nat. Mater.* **2006**, *6*, 652–655.
- (23) Yavari, F.; Castillo, E.; Gullapalli, H.; Ajayan, P. M.; Koratkar, N. High sensitivity detection of NO₂ and NH₃ in air using chemical vapor deposition grown graphene. *Appl. Phys. Lett.* **2012**, *100*, 203120.
- (24) Neto, A. H. C.; Guinea, F.; Peres, N. M. R.; Novoselov, K. S.; Geim, A. K. The electronic properties of graphene. *Rev. Mod. Phys.* **2009**, *81*, 109–162.
- (25) KS, N.; D, J.; F, S.; TJ, B.; VV, K.; SV, M.; AK, G. Two-dimensional atomic crystals. *Proc. Natl. Acad. Sci. U. S. A.* **2005**, *102*, 10451–10453.
- (26) Berger, C. *Electronic Confinement and Coherence in Patterned Epitaxial Graphene*, APS March Meeting, 2007; pp 1191–1196.
- (27) First, P. N.; de Heer, W. A.; Seyller, T.; Berger, C.; Strosio, J. A.; Moon, J.-S. Epitaxial Graphenes on Silicon Carbide. *MRS Bull.* **2010**, *35*, 296–305.
- (28) Melios, C.; Panchal, V.; Edmonds, K.; Lartsev, A.; Yakimova, R.; Kazakova, O. Detection of ultra-low concentration NO₂ in complex environment using epitaxial graphene sensors. *ACS Sens.* **2018**, *3*, 1666–1674.

- (29) Eriksson, J.; Puglisi, D.; Kang, Y. H.; Yakimova, R.; Lloyd Spetz, A. Adjusting the electronic properties and gas reactivity of epitaxial graphene by thin surface metallization. *Phys. B* **2014**, *439*, 105–108.
- (30) Phan, D.-T.; Chung, G.-S. A novel Pd nanocube–graphene hybrid for hydrogen detection. *Sens. Actuators, B* **2014**, *199*, 354–360.
- (31) Tran, Q. T.; Hoa, H. T. M.; Yoo, D.-H.; Cuong, T. V.; Hur, S. H.; Chung, J. S.; Kim, E. J.; Kohl, P. A. Reduced graphene oxide as an over-coating layer on silver nanostructures for detecting NH₃ gas at room temperature. *Sens. Actuators, B* **2014**, *194*, 45–50.
- (32) Su, Y.; Xie, G.; Chen, J.; Du, H.; Zhang, H.; Yuan, Z.; Ye, Z.; Du, X.; Tai, H.; Jiang, Y. Reduced graphene oxide–polyethylene oxide hybrid films for toluene sensing at room temperature. *RSC Adv.* **2016**, *6*, 97840–97847.
- (33) Won, S. J.; Alexander, K.; Magnuson, C. W.; Yufeng, H.; Samir, A.; Jinho, A.; Swan, A. K.; Goldberg, B. B.; Ruoff, R. S. Transfer of CVD-grown monolayer graphene onto arbitrary substrates. *ACS Nano* **2011**, *5*, 6916–6924.
- (34) Losurdo, M.; Giangregorio, M. M.; Pio, C.; Giovanni, B. Graphene CVD growth on copper and nickel: role of hydrogen in kinetics and structure. *Phys. Chem. Chem. Phys.* **2011**, *13*, 20836–20843.
- (35) Li, X.; Cai, W.; An, J.; Kim, S.; Nah, J.; Yang, D.; Piner, R.; Velamakanni, A.; Jung, I.; Tutuc, E.; Banerjee, S. K.; Colombo, L.; Ruoff, R. S. Large-area synthesis of high-quality and uniform graphene films on copper foils. *Science* **2009**, *324*, 1312.
- (36) Espid, E.; Taghipour, F. Development of highly sensitive ZnO/In₂O₃ composite gas sensor activated by UV-LED. *Sens. Actuators, B* **2017**, *241*, 828–839.
- (37) Su, Y.; Xie, G.; Tai, H.; Li, S.; Yang, B.; Wang, S.; Zhang, Q.; Du, H.; Zhang, H.; Du, X.; Jiang, Y. Self-powered room temperature NO₂ detection driven by triboelectric nanogenerator under UV illumination. *Nano Energy* **2018**, *47*, 316–324.
- (38) Chen, Y.; Li, X.; Li, X.; Wang, J.; Tang, Z. UV activated hollow ZnO microspheres for selective ethanol sensors at low temperatures. *Sens. Actuators, B* **2016**, *232*, 158–164.
- (39) Zhang, Q.; Xie, G.; Xu, M.; Su, Y.; Tai, H.; Du, H.; Jiang, Y. Visible light-assisted room temperature gas sensing with ZnO-Ag heterostructure nanoparticles. *Sens. Actuators, B* **2018**, *259*, 269–281.
- (40) Cançado, L. G.; Jorio, A.; Ferreira, E. H.; Stavale, F.; Achete, C. A.; Capaz, R. B.; Moutinho, M. V.; Lombardo, A.; Kulmala, T. S.; Ferrari, A. C. Quantifying Defects in Graphene via Raman Spectroscopy at Different Excitation Energies. *Nano Lett.* **2012**, *11*, 3190–3196.
- (41) Eckmann, A.; Felten, A.; Mishchenko, A.; Britnell, L.; Krupke, R.; Novoselov, K. S.; Casiraghi, C. Probing the nature of defects in graphene by Raman spectroscopy. *Nano Lett.* **2012**, *12*, 3925–3930.
- (42) Ferrari, A. C.; Meyer, J. C.; Scardaci, V.; Casiraghi, C.; Lazzeri, M.; Mauri, F.; Piscanec, S.; Jiang, D.; Novoselov, K. S.; Roth, S.; Geim, A. K. Raman Spectrum of Graphene and Graphene Layers. *Phys. Rev. Lett.* **2006**, *97*, 187401.
- (43) Kim, K. S.; Zhao, Y.; Jang, H.; Lee, S. Y.; Kim, J. M.; Kim, K. S.; Ahn, J.-H.; Kim, P.; Choi, J.-Y.; Hong, B. H. Large-scale pattern growth of graphene films for stretchable transparent electrodes. *Nature* **2009**, *457*, 706.
- (44) Bai, J.; Duan, X.; Huang, Y. Rational Fabrication of Graphene Nanoribbons Using a Nanowire Etch Mask. *Nano Lett.* **2009**, *9*, 2083–2087.
- (45) Chen, J.-H.; Jang, C.; Adam, S.; Fuhrer, M. S.; Williams, E. D.; Ishigami, M. Charged-impurity scattering in graphene. *Nat. Phys.* **2008**, *4*, 377.
- (46) Tan, C.; Huang, X.; Zhang, H. Synthesis and applications of graphene-based noble metal nanostructures. *Mater. Today.* **2013**, *16*, 29–36.
- (47) Kim, I.-D.; Choi, S.-J.; Cho, H.-J., Graphene-Based Composite Materials for Chemical Sensor Application. In *Electrospinning for High Performance Sensors*; Macagnano, A., Zampetti, E., Kny, E., Eds.; Springer International Publishing: Cham, 2015; pp 65–101.
- (48) Min, G. C.; Kim, D. H.; Dong, K. S.; Kim, T.; Im, H. U.; Lee, H. M.; Yoo, J. B.; Hong, S. H.; Kang, T. J.; Yong, H. K. Flexible hydrogen sensors using graphene with palladium nanoparticle decoration. *Sens. Actuators, B* **2012**, *169*, 387–392.
- (49) Yamamoto, S.; Takeuchi, K.; Hamamoto, Y.; Liu, R.-y.; Shiozawa, Y.; Koitaya, T.; Someya, T.; Tashima, K.; Fukidome, H.; Mukai, K.; Yoshimoto, S.; Suemitsu, M.; Morikawa, Y.; Yoshinobu, J.; Matsuda, I. Enhancement of CO₂ adsorption on oxygen-functionalized epitaxial graphene surface at near-ambient conditions. *Phys. Chem. Chem. Phys.* **2018**, *20*, 19532–19538.
- (50) Kodu, M.; Berholts, A.; Kahro, T.; Avarmaa, T.; Kasikov, A.; Niilisk, A.; Alles, H.; Jaaniso, R. Highly sensitive NO₂ sensors by pulsed laser deposition on graphene. *Appl. Phys. Lett.* **2016**, *109*, 1530–1534.
- (51) Leenaerts, O.; Partoens, B.; Peeters, F. M. Adsorption of H₂O, NH₃, CO, NO₂, and NO on graphene: A first-principles study. *Phys. Rev. B: Condens. Matter Mater. Phys.* **2008**, *77*, 125416.
- (52) Ren, Y.; Zhu, C.; Cai, W.; Li, H.; Ji, H.; Kholmanov, I.; Wu, Y.; Piner, R. D.; Ruoff, R. S. Detection of sulfur dioxide gas with graphene field effect transistor. *Appl. Phys. Lett.* **2012**, *100*, 163114.
- (53) Gütés, A.; Hsia, B.; Allen, S.; Willi, M.; Alex, Z.; Carlo, C.; Roya, M. Graphene decoration with metal nanoparticles: towards easy integration for sensing applications. *Nanoscale* **2012**, *4*, 438–440.
- (54) Berholts, A.; Kahro, T.; Floren, A.; Alles, H.; Jaaniso, R. Photo-activated oxygen sensitivity of graphene at room temperature. *Appl. Phys. Lett.* **2014**, *105*, 163111.
- (55) Kong, L.; Enders, A.; Rahman, T. S.; Dowben, P. A. Molecular adsorption on graphene. *J. Phys.: Condens. Matter* **2014**, *26*, 443001.
- (56) Du, H.; Xie, G.; Su, Y.; Tai, H.; Du, X.; Yu, H.; Zhang, Q. A New Model and Its Application for the Dynamic Response of RGO Resistive Gas Sensor. *Sensors* **2019**, *19*, 889.
- (57) Su, Y.; Xie, G.; Wang, S.; Tai, H.; Zhang, Q.; Du, H.; Zhang, H.; Du, X.; Jiang, Y. Novel high-performance self-powered humidity detection enabled by triboelectric effect. *Sens. Actuators, B* **2017**, *251*, 144–152.
- (58) Chung, M. G.; Kim, D. H.; Lee, H. M.; Kim, T.; Choi, J. H.; Seo, D. K.; Yoo, J.-B.; Hong, S.-H.; Kang, T. J.; Kim, Y. H. Highly sensitive NO₂ gas sensor based on ozone treated graphene. *Sens. Actuators, B* **2012**, *166–167*, 172–176.
- (59) Wu, Z.; Chen, X.; Zhu, S.; Zhou, Z.; Yao, Y.; Quan, W.; Liu, B. Enhanced sensitivity of ammonia sensor using graphene/polyaniline nanocomposite. *Sens. Actuators, B* **2013**, *178*, 485–493.
- (60) Lu, G.; Park, S.; Kehan, Y.; Ruoff, R. S.; Ocola, L. E.; Daniel, R.; Junhong, C. Toward practical gas sensing with highly reduced graphene oxide: a new signal processing method to circumvent run-to-run and device-to-device variations. *ACS Nano* **2011**, *5*, 1154–1164.
- (61) Park, S.; Park, M.; Kim, S.; Katz, J. S.; Park, J.; Ahn, C. H.; Kodama, T.; Asheghi, M.; Kenny, T. W.; Goodson, K. E. NO₂ gas sensor based on hydrogenated graphene. *Appl. Phys. Lett.* **2017**, *111*, 213102.
- (62) Kumar, R.; Goel, N.; Kumar, M. UV-Activated MoS₂ Based Fast and Reversible NO₂ Sensor at Room Temperature. *ACS Sens.* **2017**, *2*, 1744–1752.
- (63) Espid, E.; Taghipour, F. UV-LED Photo-activated Chemical Gas Sensors: A Review. *Crit. Rev. Solid State Mater. Sci.* **2017**, *42*, 416–432.
- (64) Zhou, Y.; Zou, C.; Lin, X.; Guo, Y. UV light activated NO₂ gas sensing based on Au nanoparticles decorated few-layer MoS₂ thin film at room temperature. *Appl. Phys. Lett.* **2018**, *113*, 082103.
- (65) Rigoni, F.; Maiti, R.; Baratto, C.; Donarelli, M.; Macleod, J.; Gupta, B.; Lyu, M.; Ponzoni, A.; Sberveglieri, G.; Motta, N.; Faglia, G. Transfer of CVD-grown graphene for room temperature gas sensors. *Nanotechnology* **2017**, *28*, 414001.
- (66) Zhou, Y.; Gao, C.; Guo, Y. UV assisted ultrasensitive trace NO₂ gas sensing based on few-layer MoS₂ nanosheet-ZnO nanowire heterojunctions at room temperature. *J. Mater. Chem. A* **2018**, *6*, 10286–10296.
- (67) Jeon, J.-Y.; Kang, B.-C.; Byun, Y. T.; Ha, T.-J. High-performance gas sensors based on single-wall carbon nanotube

random networks for the detection of nitric oxide down to the ppb-level. *Nanoscale* **2019**, *11*, 1587–1594.

(68) Cui, S.; Pu, H.; Wells, S. A.; Wen, Z.; Mao, S.; Chang, J.; Hersam, M. C.; Chen, J. Ultrahigh sensitivity and layer-dependent sensing performance of phosphorene-based gas sensors. *Nat. Commun.* **2015**, *6*, 8632.

(69) Hu, J.; Zou, C.; Su, Y.; Ming, L.; Zhang, Y. Enhanced NO₂ sensing performance of reduced graphene oxide by: In situ anchoring carbon dots. *J. Mater. Chem. C* **2017**, *5*, 6862–6871.

(70) Wang, T.; Hao, J.; Zheng, S.; Quan, S.; Di, Z.; You, W. Highly sensitive and rapidly responding room-temperature NO₂ gas sensors based on WO₃ nanorods/sulfonated graphene nanocomposites. *Nano Res.* **2017**, *11*, 791–803.

(71) Yuan, W.; Huang, L.; Zhou, Q.; Shi, G. Ultrasensitive and Selective Nitrogen Dioxide Sensor Based on Self-Assembled Graphene/Polymer Composite Nanofibers. *ACS Appl. Mater. Interfaces* **2014**, *6*, 17003–17008.

(72) Gu, F.; Nie, R.; Han, D.; Wang, Z. In₂O₃-graphene nanocomposite based gas sensor for selective detection of NO₂ at room temperature. *Sens. Actuators, B* **2015**, *219*, 94–99.

(73) Currie, L. A. Nomenclature in evaluation of analytical methods including detection and quantification capabilities (IUPAC Recommendations 1995). *Pure Appl. Chem.* **1995**, *67*, 1699–1723.

(74) Zhou, Y.; Liu, G.; Xiangyi, Z.; Yongcai, G. Ultra-sensitive NO₂ gas sensing based on rGO/MoS₂ nanocomposite film at low temperature. *Sens. Actuators, B* **2017**, *251*, 280–290.

(75) Yang, S.; Jiang, C.; Wei, S.-h. Gas sensing in 2D materials. *Appl. Phys. Rev.* **2017**, *4*, 021304.

(76) Wehling, T. O.; Katsnelson, M. I.; Lichtenstein, A. I. Adsorbates on graphene: Impurity states and electron scattering. *Chem. Phys. Lett.* **2009**, *476*, 125–134.

(77) Bruch, L. W.; Cole, M. W.; Kim, H.-Y. Transitions of gases physisorbed on graphene. *J. Phys.: Condens. Matter* **2010**, *22*, 304001.

(78) Alfano, B.; Massera, E.; Miglietta, M. L.; Polichetti, T.; Schiattarella, C.; Francia, G. D. *Graphene Decoration for Gas Detection; Aisem Conference on Sensors and Microsystems*, 2017; pp 35–40.

(79) Park, S.; An, S.; Mun, Y.; Lee, C. UV-Enhanced NO₂ Gas Sensing Properties of SnO₂-Core/ZnO-Shell Nanowires at Room Temperature. *ACS Appl. Mater. Interfaces* **2013**, *5*, 4285–4292.

(80) Jiménez-Cadena, G.; Riu, J.; F Xavier, R. Gas sensors based on nanostructured materials. *Analyst* **2007**, *132*, 1083–1099.

(81) Li, X.; Li, X.; Wang, J.; Lin, S. Highly sensitive and selective room-temperature formaldehyde sensors using hollow TiO₂ microspheres. *Sens. Actuators, B* **2015**, *219*, 158–163.

(82) Wang, P.; Fu, Y.; Yu, B.; Zhao, Y.; Xing, L.; Xue, X. Realizing room-temperature self-powered ethanol sensing of ZnO nanowire arrays by combining their piezoelectric, photoelectric and gas sensing characteristics. *J. Mater. Chem. A* **2015**, *3*, 3529–3535.